



Measurements of activity coefficients at infinite dilution of organic solutes and water on polar imidazolium-based ionic liquids



Mónia A.R. Martins^{a,b}, João A.P. Coutinho^a, Simão P. Pinho^{c,*}, Urszula Domańska^b

^a Departamento de Química, CICECO, Universidade de Aveiro, 3810-193 Aveiro, Portugal

^b Physical Chemistry Department, Warsaw University of Technology, 00-661 Warsaw, Poland

^c Associate Laboratory LSRE/LCM, Departamento de Tecnologia Química e Biológica, Instituto Politécnico de Bragança, 5301-857 Bragança, Portugal

ARTICLE INFO

Article history:

Received 9 February 2015

Received in revised form 16 July 2015

Accepted 29 July 2015

Available online 3 August 2015

Keywords:

Ionic liquids

Organic solutes

(Gas + liquid) partition coefficients

Selectivity

ABSTRACT

The activity coefficients at infinite dilution, γ_{13}^{∞} , of 55 organic solutes and water in three ionic liquids with the common cation 1-butyl-3-methylimidazolium and the polar anions Cl^- , $[\text{CH}_3\text{SO}_3]^-$ and $[(\text{CH}_3)_2\text{PO}_4]^-$, were determined by (gas + liquid) chromatography at four temperatures in the range (358.15 to 388.15) K for alcohols and water, and $T = (398.15 \text{ to } 428.15) \text{ K}$ for the other organic solutes including alkanes, cycloalkanes, alkenes, cycloalkenes, alkynes, ketones, ethers, cyclic ethers, aromatic hydrocarbons, esters, butyraldehyde, acetonitrile, pyridine, 1-nitropropane and thiophene. From the experimental γ_{13}^{∞} values, the partial molar excess Gibbs free energy, $\bar{G}_m^{E,\infty}$, enthalpy $\bar{H}_m^{E,\infty}$, and entropy $\bar{S}_m^{E,\infty}$, at infinite dilution, were estimated in order to provide more information about the interactions between the solutes and the ILs. Moreover, densities were measured and (gas + liquid) partition coefficients (K_1) calculated. Selectivities at infinite dilution for some separation problems such as octane/benzene, cyclohexane/benzene and cyclohexane/thiophene were calculated using the measured γ_{13}^{∞} , and compared with literature values for *N*-methyl-2-pyrrolidinone (NMP), sulfolane, and other ionic liquids with a common cation or anion of the ILs here studied. From the obtained infinite dilution selectivities and capacities, it can be concluded that the ILs studied may replace conventional entrainers applied for the separation processes of aliphatic/aromatic hydrocarbons.

© 2015 Elsevier Ltd. All rights reserved.

1. Introduction

Due to their exceptional properties, namely chemical and thermal stability, non-volatility, adjustable miscibility and polarity [1], ionic liquids (ILs) have emerged as potential substitutes for organic solvents and have found applications in a variety of fields as organic synthesis, catalysis, biocatalysis, electrochemistry, and separation technology, at both laboratory level and industrial scale [2–4]. In separations, further applications are related to the pharmaceutical, environmental and biomedical industries, where ILs have been used for (liquid + liquid) or supported liquid membrane extraction, as additives and as stationary phases in chromatography [4,5].

In order to replace a conventional separation process by another that uses ILs, this must be more performant and cost-effective, what is, in general, difficult. Due to their cost, higher than for common solvents, the main challenges in applying ionic liquids are related to their recovery and reutilization. Related to this, as some

will inevitably be lost in the process is their biodegradability and (eco)toxicity in the aquatic compartment. Ionic liquids are being considered as designer solvents. Therefore, a good knowledge of their (physical + chemical) properties, and phase equilibria, is a fundamental step for the design and optimization of industrial processes [1].

To fully exploit the ionic liquids potential as solvents in separation processes, the importance of (ILs + organic solutes) interactions is well recognized [6]. The understanding of such interactions can be derived from physico-chemical measurements such as solubilities [7,8], activity coefficients of solutes at infinite dilution (γ_{13}^{∞}) [9–12], molecular simulation [13,14], spectroscopic techniques [15–17], (vapor + liquid) equilibrium (VLE) data [18,19] and (liquid + liquid) equilibrium (LLE) data [20,21], as well as from thermodynamic models such as equations of state [22] or from COSMO [19,20].

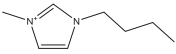
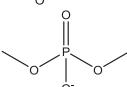
Very useful for screening purposes, the activity coefficient of solutes at infinite dilution are related to the relative strength of intermolecular interaction with the ionic liquid, being the lowest values usually observed for alkynes and polar substances such as alcohols, ketones and ethers; a result from the hydrogen bonding,

* Corresponding author. Tel.: +351 273303086; fax: +351 273313051.

E-mail address: spinho@ipb.pt (S.P. Pinho).

TABLE 1

Studied ionic liquids: name, structure, abbreviation, source, molar mass (M), melting point (T_{MP}) and purity.

Chemical formula		Chemical name	Supplier	M ($\text{g} \cdot \text{mol}^{-1}$)	T_{MP} (K)	Purity (mass%)
Cation	Anion					
	Cl^-	1-butyl-3-methylimidazolium chloride, [C ₄ mim]Cl	IoLiTec	174.67	341.95 ^a	99
		1-butyl-3-methylimidazolium methanesulfonate, [C ₄ mim][CH ₃ SO ₃]	IoLiTec	234.32	≈353.15 ^b	99
		1-butyl-3-methylimidazolium dimethyl phosphate, [C ₄ mim][(CH ₃) ₂ PO ₄]	IoLiTec	264.26	n.a. ^c	98

^a Ref. [56].^b Ref. [57].^c Not available.

the $\pi - \pi$, $\sigma - \pi$, or other strong interactions [23]. γ_{13}^{∞} can be determined from retention times using (gas + liquid) chromatography (GLC) [24–26] or through the diluter technique [27,28]. In the GLC method, the chromatographic column is coated with the ionic liquid and the solutes introduced with a carrier gas. The solutes retention times are a measure of the strength of interaction, *i.e.*, the infinite dilution activity coefficients, of the solute in the ionic liquids. This technique work for solutes that are retained by the IL more strongly than by the carrier gas (usually helium) [29].

A perspective of this work is the separation of aromatic from aliphatic hydrocarbons, and desulphurization processes. The separation of aromatic hydrocarbons from C4 to C10 aliphatic hydrocarbon mixtures is challenging since these hydrocarbons have boiling points in a close range, and several combinations form azeotropes. The discussion on the desulphurization, or denitrogenation of fuels is also important nowadays. Thus, in this work, the activity coefficients at infinite dilution of 55 organic solutes, including alkanes, cycloalkanes, alkenes, cycloalkenes, alkynes, ketones, ethers, cyclic ethers, aromatic hydrocarbons, esters, alcohols, butyraldehyde, acetonitrile, pyridine, 1-nitropropane and thiophene; and water, in the ionic liquids 1-butyl-3-methylimidazolium chloride, [C₄mim]Cl; 1-butyl-3-methylimidazolium dimethyl phosphate, [C₄mim][(CH₃)₂PO₄]; and 1-butyl-3-methylimidazolium methanesulfonate, [C₄mim][CH₃SO₃], are reported. For methodological reasons, the organic solutes were selected taking into account their boiling points (between $T = 304.12$ and 428.76 K), hence allowing for equilibration at elevated temperatures and reducing ionic liquid viscosities, while avoiding their decomposition. Ionic liquids with same cation and different anions were chosen in order to rationalize the effect of changes in the structures, evaluating polarity, as these anions present solvatochromic parameters reflecting very high hydrogen-bond acceptor ability. Values were determined by (gas + liquid) chromatography at $T = 10$ K intervals in range $T = (358.15$ to $388.15)$ K for alcohols and water, and $T = (398.15$ to $428.15)$ K for the other organic solutes. The ILs density as a function of temperature was measured in order to calculate the (gas + liquid) partition coefficients, K_L . Excess thermodynamic properties at infinite dilution, and at $T = 358.15$ K, are also discussed. Comparisons with previously published imidazolium-based ILs are addressed.

2. Experimental

2.1. Chemicals

The chemical structure and some of the properties of the studied ILs are presented in table 1. Organic solutes source and purity can be found in table S1 of Supporting Information. In order to reduce the water and volatile compounds individual samples of

ILs were dried under vacuum at 0.1 Pa and constant stirring at $T = 353$ K, for a minimum of 48 h. After, the purity of each ionic liquid was further checked by ¹H, ¹³C, and ¹⁹F NMR spectra. Additional drying was applied keeping the ILs during 72 h at $T = 300$ K under reduced pressure to remove volatile impurities and traces of water. The water content of the dried ILs was determined using the Karl Fischer titration technique (method TitroLine KF). Samples were dissolved in dry methanol and titrated with a step of 2.5 μL . The analysis showed that the water content was found to be below 300 ppm for all samples. The organic solutes were used without further purification once GLC technique separates impurities in the column. The water used in the measurements was distilled and filtered, presenting a final mass fraction purity higher than 0.999, being the analysis performed through density measurement.

2.2. Apparatus and experimental procedure

The activity coefficients at infinite dilution were determined using the GLC method previously presented in detail [23,30–33]. Experiments were carried out using a PerkinElmer Clarus 500 gas chromatograph equipped with a heated on-column injector and a thermal conductivity detector (TCD). The injector and detector temperatures were kept at 473.15 K during the experiments, value above the boiling point of the solutes. Helium was used as the carrier gas and the exit gas flow rates were measured with one Agilent Precision Gas Flow Meter placed on the outside, after the detector, with an uncertainty of ± 0.1 $\text{cm}^3 \cdot \text{min}^{-1}$. The inlet pressure, P_i , was measured by a pressure gauge installed on the gas chromatograph with an uncertainty of ± 0.1 kPa and the outlet pressure, P_o , was measured using the same Agilent Precision Gas Flow Meter with an uncertainty of ± 0.07 kPa. The settled inlet pressure was 10 kPa for alkanes, cycloalkanes, alkenes, cycloalkenes, alkynes and ethers; 60 kPa for aromatic hydrocarbons, ketones, cyclic ethers, esters, butyraldehyde, acetonitrile, pyridine, 1-nitropropane and thiophene; and 80 kPa for alcohols and water. The outlet pressure ranged between [98.18 and 101.08] kPa. Data were collected and processed using the TotalChrom Workstation software.

Column preparation and packing method have been described in previous works [34,35] and will be only briefly described here. Column packing containing between (45 and 55)% IL stationary phase coated onto a (100 to 120) mesh Chromosorb W/AW – DMCS solid support material (supplied by Sigma-Aldrich), were prepared by the rotary evaporation technique. High amounts of ILs were used to avoid possible residual adsorption effects of the solutes on the solid support. Each IL was dissolved in methanol and dispersed in Chromosorb. After coating, the mixture was shaken, and vacuum-assisted rotary evaporation was used to remove

TABLE 2
Activity coefficients at infinite dilution of organic compounds and water in ILs, at different temperatures.^a

Organic solutes	[C ₄ mim]Cl ^b				[C ₄ mim][CH ₃ SO ₃] ^c				[C ₄ mim][(CH ₃) ₂ PO ₄] ^d			
	T/K	358.15	368.15	378.15	388.15	358.15	368.15	378.15	388.15	358.15	368.15	378.15
Octane	330.66	302.07	268.50	258.36	170.84	164.58	159.96	155.32	47.90	46.22	44.57	43.35
Nonane	475.82	432.95	393.64	375.50	250.53	239.46	229.20	223.29	67.86	63.95	61.45	59.15
Decane	704.04	637.87	579.72	560.12	371.49	351.76	340.15	324.31	93.39	88.52	84.67	81.58
Cyclopentane	38.69	36.24	33.50	31.83	23.85	23.70	23.50	23.26	8.76	8.59	8.41	8.33
Cyclohexane	54.69	50.90	47.36	44.92	35.18	34.49	33.90	33.81	12.29	11.88	11.64	11.45
Methylcyclohexane	84.25	79.00	73.02	69.85	52.79	51.70	50.88	50.40	17.38	16.78	16.40	16.07
Cycloheptane	62.67	58.82	55.41	53.57	44.21	43.33	42.59	42.25	15.14	14.64	14.26	14.00
Cyclooctane	79.55	75.40	71.10	68.62	57.11	55.66	54.42	53.60	18.77	18.24	17.72	17.33
Hex-1-ene	61.71	57.87	53.94	51.97	39.66	39.99	40.01	40.26	13.89	13.71	13.40	13.20
Hept-1-ene	88.90	83.76	79.33	77.17	59.23	58.91	58.68	58.03	19.61	19.38	19.15	18.91
Oct-1-ene	141.84	134.44	125.75	122.50	88.06	86.76	86.48	85.64	27.49	26.95	26.46	26.22
Dec-1-ene	322.82	305.86	284.63	277.46	192.88	187.08	181.89	179.06	53.50	52.23	50.44	49.24
Cyclohexene	22.84	22.30	21.48	21.31	18.44	18.59	18.73	19.00	7.15	7.13	7.11	7.11
Pent-1-yne	4.89	5.25	5.51	5.78	5.46	5.84	6.26	6.67	2.18	2.32	2.46	2.60
Hex-1-yne	7.33	7.85	8.19	8.61	8.02	8.52	9.06	9.64	3.01	3.22	3.39	3.57
Hept-1-yne	11.63	12.30	12.74	13.33	11.97	12.64	13.34	14.11	4.21	4.48	4.70	4.93
Oct-1-yne	18.32	19.20	19.73	20.45	17.77	18.58	19.47	20.39	6.04	6.22	6.48	6.74
Acetone	3.05	3.12	3.17	3.27	2.06	2.12	2.22	2.30	1.92	1.96	2.02	2.10
Pentan-2-one	7.59	7.71	7.78	8.01	4.50	4.59	4.76	4.91	3.63	3.70	3.78	3.94
Pentan-3-one	7.60	7.72	7.78	7.97	4.68	4.79	4.88	5.09	3.73	3.81	3.89	4.04
MTBE	24.61	23.80	23.02	22.85	16.97	17.39	17.90	18.55	7.17	7.35	7.48	7.66
TAME	33.96	33.14	32.18	32.06	23.82	24.18	24.67	25.26	9.50	9.61	9.66	9.75
ETBE	64.78	59.34	55.67	53.32	35.29	35.59	36.10	36.62	12.75	12.78	12.89	12.95
Diethyl ether	19.27	18.93	18.36	18.39	14.69	14.91	14.98	15.32	6.21	6.30	6.39	6.48
Di- <i>n</i> -propyl ether	57.40	55.26	52.78	51.93	38.11	38.73	38.94	39.41	13.95	13.73	13.55	13.42
Di- <i>iso</i> -propyl ether	78.53	71.67	63.98	59.12	40.59	40.79	40.79	41.19	14.39	14.27	14.22	14.12
Di- <i>n</i> -butyl ether	130.04	124.82	118.31	116.17	83.87	82.13	81.55	80.53	26.78	26.23	25.90	25.52
THF	5.66	5.67	5.67	5.70	3.41	3.48	3.59	3.72	2.79	2.84	2.89	3.02
1,4-Dioxane	3.47	3.55	3.65	3.74	2.33	2.41	2.49	2.62	2.13	2.19	2.25	2.37
Benzene	4.51	4.59	4.72	4.82	3.08	3.19	3.29	3.46	2.33	2.41	2.49	2.63
Toluene	7.78	7.91	8.09	8.36	5.32	5.45	5.68	5.84	3.86	3.99	4.09	4.29
Ethylbenzene	13.15	13.25	13.51	13.73	8.45	8.61	8.76	9.05	5.73	5.87	5.97	6.26
<i>o</i> -Xylene	11.55	11.72	11.93	12.28	7.64	7.79	7.99	8.21	5.54	5.70	5.79	6.03
<i>m</i> -Xylene	14.31	14.50	14.69	15.02	9.27	9.43	9.57	9.92	6.49	6.60	6.73	7.00
<i>p</i> -Xylene	13.63	13.72	14.00	14.29	9.03	9.20	9.37	9.71	6.31	6.44	6.59	6.86
Styrene	4.96	5.18	5.42	5.73	3.79	3.96	4.20	4.40	2.79	2.93	3.06	3.26
α -Methylstyrene	9.01	9.33	9.83	10.34	6.43	6.71	6.96	7.41	4.57	4.77	4.98	5.29
Methyl acetate	4.82	4.89	5.01	5.09	2.94	3.03	3.14	3.33	2.58	2.65	2.73	2.85
Ethyl acetate	9.02	9.06	9.10	9.16	4.76	4.88	5.00	5.28	3.81	3.91	4.01	4.18
Methyl propanoate	8.00	8.09	8.20	8.31	4.43	4.56	4.68	4.90	3.56	3.65	3.76	3.93
Methyl butanoate	12.30	12.43	12.57	12.69	6.79	7.21	7.39	7.84	4.93	5.04	5.17	5.39
Vinyl acetate	5.66	5.74	5.86	6.05	3.47	3.58	3.76	3.92	2.79	2.88	2.99	3.13
Butyraldehyde	5.24	5.31	5.43	5.54	3.33	3.44	3.58	3.74	2.66	2.74	2.82	2.97
Acetonitrile	1.12	1.16	1.21	1.28	0.99	1.03	1.08	1.12	0.88	0.92	0.95	1.00
Pyridine	1.47	1.55	1.64	1.78	1.093	1.080	1.061	1.047	1.18	1.23	1.28	1.35
1-Nitropropane	2.51	2.61	2.69	2.80	1.89	1.96	2.02	2.13	1.50	1.56	1.62	1.72
Thiophene	2.04	2.16	2.27	2.41	1.72	1.81	1.94	2.05	1.24	1.35	1.43	1.53
T/K	398.15	408.15	418.15	428.15	398.15	408.15	418.15	428.15	398.15	408.15	418.15	428.15
Methanol	0.156	0.166	0.176	0.191	0.325	0.340	0.357	0.373	0.097	0.105	0.115	0.125
Ethanol	0.297	0.313	0.332	0.353	0.533	0.553	0.576	0.599	0.160	0.173	0.189	0.205
Propan-1-ol	0.408	0.434	0.464	0.501	0.711	0.744	0.783	0.823	0.197	0.218	0.239	0.264
Propan-2-ol	0.542	0.577	0.619	0.668	0.835	0.878	0.928	0.976	0.256	0.282	0.311	0.344
2-Methyl-propan-1-ol	0.540	0.576	0.615	0.665	0.893	0.938	0.991	1.042	0.230	0.254	0.281	0.313
Butan-1-ol	0.558	0.594	0.635	0.680	0.937	0.984	1.024	1.071	0.247	0.271	0.299	0.324
Butan-2-ol	0.749	0.804	0.865	0.931	1.114	1.181	1.255	1.333	0.327	0.365	0.406	0.451
<i>tert</i> -Butanol	0.987	1.067	1.159	1.269	1.285	1.385	1.483	1.594	0.419	0.471	0.527	0.592
Water	0.070	0.077	0.085	0.094	0.200	0.214	0.228	0.239	0.073	0.081	0.092	0.101

^a Standard uncertainties are: $u(\gamma_{13}^{\infty}) = 3\%$ and $u(T) = 0.02$ K.

^b Packing: 52.1%, $n_3 = 17.02$ mmol.

^c Packing: 49.8%, $n_3 = 11.48$ mmol.

^d Packing: 47.3%, $n_3 = 9.39$ mmol.

the methanol. Masses of the stationary phase and of the solid support were weighed with a precision of $\pm 1 \cdot 10^{-4}$ g. Glass columns of 1 m length and 4 mm internal diameter were filled with the dry packing and placed in the chromatograph to equilibrate during 6 h, at $T = 388$ K and 60 kPa. The stream of helium gas was passed through the stationary phase for the final drying. A large amount of column packing is used also to prevent the residual adsorption of solute onto the column packing, a very important feature,

especially for alkanes. For each IL, at least two columns were prepared, with different IL packing's percentage. The deviations between the γ_{13}^{∞} in the different columns, for a given set of solutes, was always less than 3%. In general, the major contributions to the errors were from solutes with larger retention times, as alkanes, cycloalkanes, ketones and some ethers. The repeatability of γ_{13}^{∞} values from two columns were within $\pm 1.5\%$ for the vast majority of the solutes.

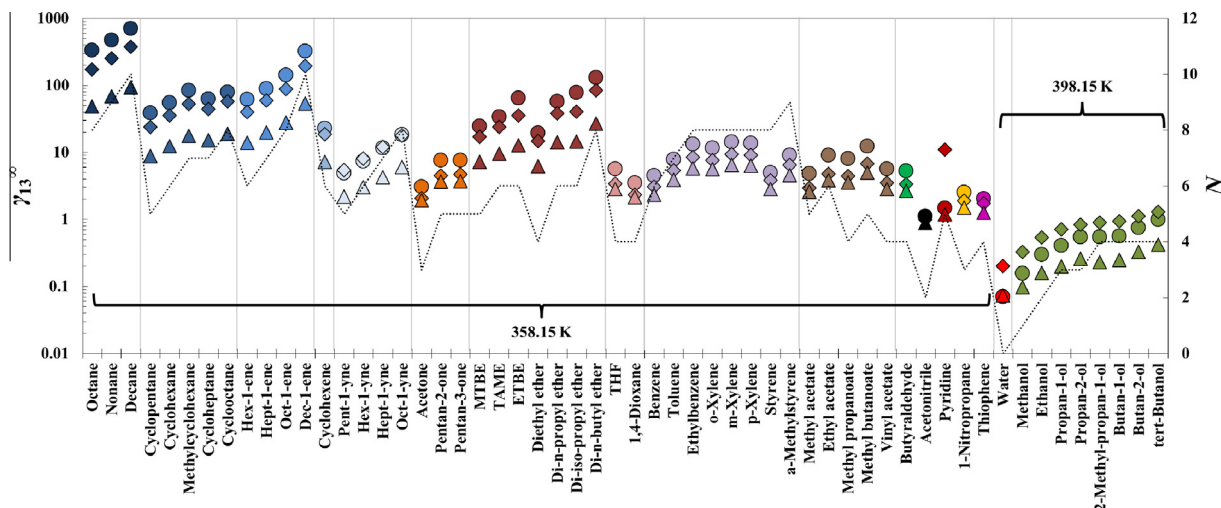


FIGURE 1. Activity coefficients at infinite dilution of several solutes in ILs, at $T = 398.15\text{ K}$ for alcohols and water, and $T = 358.15\text{ K}$ for the other organic compounds. \circ , $[\text{C}_4\text{mim}]\text{Cl}$; \diamond , $[\text{C}_4\text{mim}][\text{CH}_3\text{SO}_3]$; Δ , $[\text{C}_4\text{mim}][(\text{CH}_3)_2\text{PO}_4]$. The dotted line represents the number of carbons in the solutes structure, N . Symbols with the same color correspond to solutes of the same chemical family. (For interpretation of the references to color in this figure legend, the reader is referred to the web version of this article.)

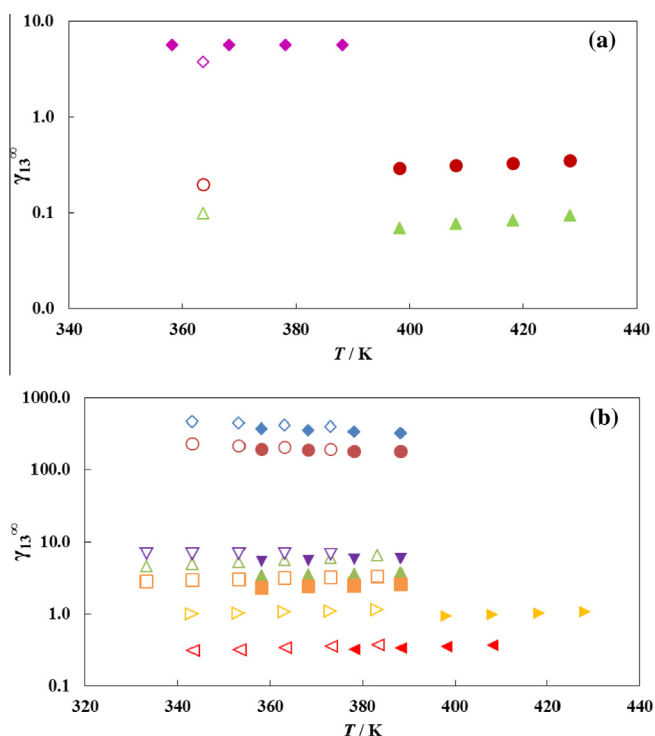


FIGURE 2. Comparison of the experimental activity coefficients at infinite dilution with values from literature for two ionic liquids: (a) $[\text{C}_4\text{mim}]\text{Cl}$, \blacklozenge THF, \bullet ethanol, \blacktriangle water (empty symbols correspond to literature data [46]); (b) $[\text{C}_4\text{mim}][\text{CH}_3\text{SO}_3]$, \blacklozenge decane, \bullet dec-1-ene, \blacktriangle THF, \blacksquare 1,4-dioxane, \blacktriangledown toluene, \blacktriangleleft methanol, \blacktriangleright butan-1-ol (empty symbols correspond to literature data [47]).

In order to measure the retention times, solutes were injected in the column in volumes of (0.01 to 0.3) μL , to be at infinite dilution conditions. In each measurement, together with the organic solutes, air was also injected, as a non-retained component. Absolute values of retention times varied between 0.30 to 64 min corresponding to di-*iso*-propyl ether and water, respectively. Each experiment was repeated at least twice to establish repeatability. The temperature of the column was maintained constant to within $\pm 0.02\text{ K}$. Measured retention times were generally

reproducible within (0.01 to 0.03) min depending upon the temperature and the individual solute. Values of the dead time, t_G , equivalent to the retention time of a completely non-retained component, in this case air, were also measured. Taking into account the solute retention times accuracy (0.001 min), and the standard deviations (in parentheses) related with: solute vapor pressures ($<5\%$), mass of the stationary phase ($<1 \cdot 10^{-4}\text{ g}$), flow rate of helium ($0.1\text{ cm}^3 \cdot \text{min}^{-1}$), inlet (0.1 kPa) and outlet (0.07 kPa) pressures, and oven temperature (0.02 K); the uncertainties in γ_1^∞ were estimated by error propagation to be less than 3%.

2.3. Density measurements

Densities measurements of the pure ILs were carried out at atmospheric pressure and in the (293.15 to 373.15) K temperature range using an automated SVM3000 Anton Paar rotational Stabinger viscometer-densimeter. The uncertainty of temperature is $\pm 0.02\text{ K}$ and the absolute uncertainty in density is $\pm 5 \cdot 10^{-4}\text{ g} \cdot \text{cm}^{-3}$. Additional details related with the equipment can be found elsewhere [36].

3. Theoretical basis

When an infinitesimal amount of solute sample is introduced into a GLC column with a non-volatile stationary phase it is possible to calculate the activity coefficient at infinite dilution for the solute (1) partitioning between the carrier gas (2) and the non-volatile liquid solvent (3) through the solute retention [25], according to the equation developed by Everett [37] and Cruickshank *et al.* [38]:

$$\ln \gamma_{13}^\infty = \ln \left(\frac{n_3 RT}{V_N P_1^*} \right) - \frac{P_1^* (B_{11} - V_1^*)}{RT} + \frac{P_0 J_2^3 (2B_{12} - V_1^\infty)}{RT} \quad (1)$$

where n_3 is the number of moles of solvent on the column packing, T is the GC oven temperature where the column is placed, V_N is the net retention volume of the solute, P_1^* is the saturated vapor pressure of the solute, B_{11} is the second virial coefficient of the pure solute, V_1^* is the molar volume of the solute, P_0 is the outlet pressure, J_2^3 is a pressure correction term, B_{12} is the mixed second virial coefficient of the solute and the carrier gas (helium), and V_1^∞ is the partial molar volume of the solute at infinite dilution in the solvent. The standard state for the solute is pure liquid at system

TABLE 3
Comparison between the activity coefficients at infinite dilution with values from literature at $T = 358.15$ K.

Ionic liquids	Octane	Cyclohexane	Benzene	Ethanol	Water	Reference
[C ₄ mim]Cl	330.7	54.7	4.5	0.22 ^a	0.04 ^a	This work
[C ₈ mim]Cl	17.1 ^a	7.8 ^a	1.3 ^a			[26]
[C ₂ mim][CH ₃ SO ₃]	275.3 ^a	45.5 ^a	4.3	0.47	0.09	[32]
[C ₂ mim][CH ₃ SO ₃]	356.7 ^a	50.5 ^a	4.1 ^a	0.36 ^a		[58]
[C ₄ mim][CH ₃ SO ₃]	170.8	35.2	3.1	0.44 ^a	0.15 ^a	This work
[C ₁ mim][(CH ₃) ₂ PO ₄]	246.1 ^a	39.6 ^a	3.8 ^a	0.13 ^a	0.05 ^a	[27]
[C ₄ mim][(CH ₃) ₂ PO ₄]	47.9	12.3	2.3	0.10 ^a	0.04 ^a	This work
[C ₂ mim][(CH ₃ CH ₂) ₂ PO ₄]	83.4 ^a	24.6 ^a	2.3 ^a			[59]
[C ₄ mim][(CH ₃ (CH ₂) ₃) ₂ PO ₄]	6.2 ^b	2.6 ^b	0.9 ^b			[60]

^a Extrapolated value.

^b Interpolated value.

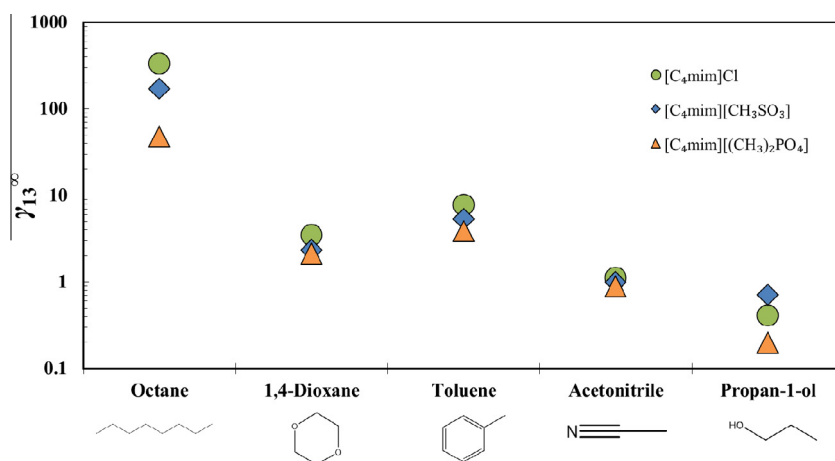


FIGURE 3. Infinite dilution activity coefficients of selected solutes in ILs, at $T = 398.15$ K for propan-1-ol, and $T = 358.15$ K for the other organic compounds.

temperature and zero pressure, and all temperature dependent properties are calculated at T .

The pressure correction term J_2^3 [39], and the net retention volume of the solute, V_N , are given by the following equations:

$$J_2^3 = \frac{2}{3} \frac{(P_i/P_0)^3 - 1}{(P_i/P_0)^2 - 1} \quad (2)$$

$$V_N = (J_2^3)^{-1} U_0 (t_R - t_G) \quad (3)$$

where t_R and t_G are the retention times for the solute and an unreturned gas (air), respectively, and U_0 is the column outlet volumetric flow rate, corrected for the vapor pressure of water by,

$$U_0 = U \left(1 - \frac{P_W}{P_0} \right) \frac{T}{T_f} \quad (4)$$

where T_f is the temperature at the column outlet, P_W is the vapor pressure of water at T_f , and U is the volumetric flow rate measured at the outlet of the column.

The temperature dependent properties required for the γ_{13}^∞ calculations were obtained using equations and constants taken from the literature [40]. The values of B_{12} were calculated using the Tsonopolous [41] correlation, applying the information also found in Poling and Prausnitz [40].

The activity coefficients at infinite dilution were determined as a function of temperature, allowing the determination of some important partial molar excess thermodynamic functions, namely

the Gibbs free energy ($\bar{G}_m^{E,\infty}$), enthalpy ($\bar{H}_m^{E,\infty}$) and entropy ($\bar{S}_m^{E,\infty}$) that will help to explore and rationalize the collected experimental information. Since the experimental activity coefficients were measured at infinite dilution, the partial molar excess properties were estimated using the following equations,

$$\bar{G}_m^{E,\infty} = RT \ln(\gamma_{13}^\infty) \quad (5)$$

$$\bar{H}_m^{E,\infty} = R \left(\frac{\partial \ln \gamma_{13}^\infty}{\partial (1/T)} \right)_{p,x} \quad (6)$$

$$\bar{S}_m^{E,\infty} = \frac{\bar{H}_m^{E,\infty} - \bar{G}_m^{E,\infty}}{T} \quad (7)$$

where subscripts p and x indicate isobaric condition and constant composition, respectively.

In order to use volatile solvents for technical purposes, their characterization is required. The partition coefficients are many times used for this purpose, since the solubility of selected substances can be predicted from them. These coefficients are also highly important in chemical engineering and environmental modeling, where the distribution of individual compounds between different organic phases and water or air, is of importance.

Aiming the determination of the order of elution from columns, partition coefficients are extracted from the retention data and many numbers have been published as a by-product of chromatographic separations, where their determination usually constitutes part of the procedure. In this work, the (gas + liquid) partition

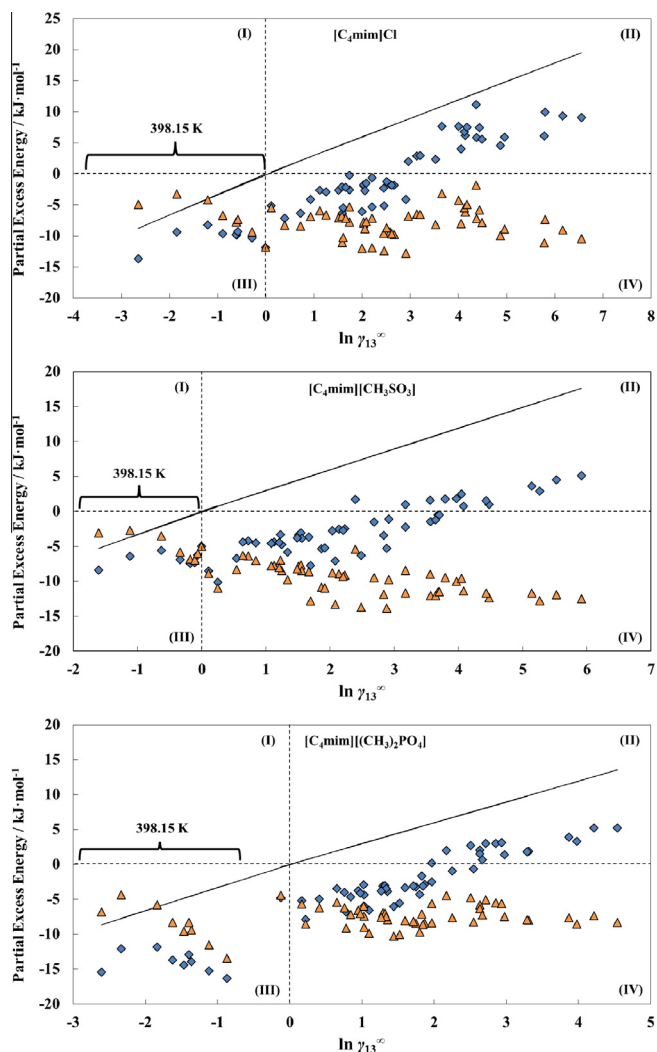


FIGURE 4. Partial molar excess energies as a function of the activity coefficients at infinite dilution of the organic solutes studied in the ILs [C₄mim]Cl, [C₄mim][CH₃SO₃] and [C₄mim][(CH₃)₂PO₄], at 358.15 and $T = 398.15$ K. The line represents $C_m^{E\infty}$ and the symbols correspond to: \diamond , $\overline{H}_m^{E\infty}$ and Δ , $T_{rep} \overline{S}_m^{E\infty}$.

coefficient $K_L = (c_1^i/c_1^f)$ for a solute partitioning between the carrier gas and the ILs was calculated from the solute retention according to the following equation [42],

$$\ln(K_L) = \ln\left(\frac{V_N \rho_3}{m_3}\right) - \frac{P_{0j}^3(2B_{12} - V_1^\infty)}{RT} \quad (8)$$

in which ρ_3 is the density of the IL and m_3 is the mass of the IL.

The selectivity between the solutes i and j , S_{ij}^∞ and the capacity k_j^∞ of the separation process are defined as follow [27]:

$$S_{ij}^\infty = \gamma_i^\infty / \gamma_j^\infty \quad (9)$$

$$k_j^\infty = 1 / \gamma_j^\infty \quad (10)$$

where j is the solute that presents the smaller infinite dilution activity coefficient in the solvent (in this work, the ILs).

4. Results and discussion

4.1. Activity coefficients at infinite dilution

The average values of the infinite dilution activity coefficients for several organic solutes, and water, in the studied ILs are presented in table 2. The measurements were carried out in the temperature range between (358.15 and 388.15) K, with intervals of $T = 10$ K. The lower temperature value was chosen regarding the ILs melting points, namely of [C₄mim]Cl and [C₄mim][CH₃SO₃], to avoid their solidification inside the column. Alcohols and water were measured between $T = (398.15$ and $428.15)$ K due to their usual longer retention times. In order to explore the data, a comparison at a fixed temperature, 358.15 K, is presented in figure 1 (for alcohols and water the values are presented at $T = 398.15$ K).

The higher the interactions between the solutes and the ionic liquids, the higher the retention times measured, and the lower the infinite dilution activity coefficients [43,44]. A global analysis of figure 1 shows that water presents the lower γ_{13}^∞ values indicating the highest interaction with the ionic liquids, what is expected since the ionic liquids were chosen with highly polar anions. Other polar solutes such as alcohols, thiophene, 1-nitropopane, pyridine and acetonitrile present also low γ_{13}^∞ values. On the opposite, alkanes and alkenes, the less polar solvents, present the weakest interactions with the ILs studied. Moreover, analyzing figure 1 it is possible to observe that the γ_{13}^∞ increases with the chain length for the alkanes, cycloalkanes, alkenes, alkynes, ketones, ethers, aromatic hydrocarbons (increasing radicals) and alcohols. The experimental values obtained in this work for aliphatic and aromatic hydrocarbons are much larger than those observed in other ILs with the same cation [24,33]. However, if compared with ILs with the same anion the γ_{13}^∞ are similar [32], indicating a dominant role of the anion on these interactions. The γ_{13}^∞ value for acetonitrile at

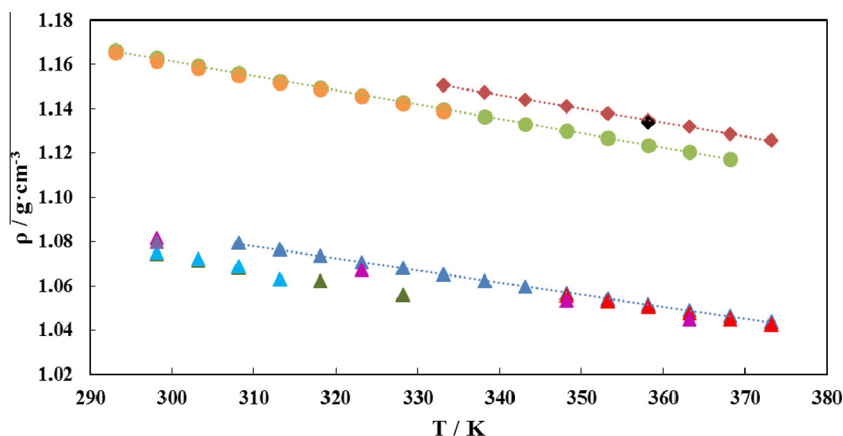


FIGURE 5. Comparison of density experimental values with literature data. Symbols: \blacktriangle [C₄mim]Cl, this work; \blacktriangle [C₄mim]Cl, [49]; \blacktriangle [C₄mim]Cl, [50]; \blacktriangle [C₄mim]Cl, [51]; \blacktriangle [C₄mim]Cl, [52]; \blacktriangle [C₄mim]Cl, [53]; \blacklozenge [C₄mim][CH₃SO₃], this work; \blacklozenge [C₄mim][CH₃SO₃], [57]; \bullet [C₄mim][(CH₃)₂PO₄], this work; \bullet [C₄mim][(CH₃)₂PO₄], [48].

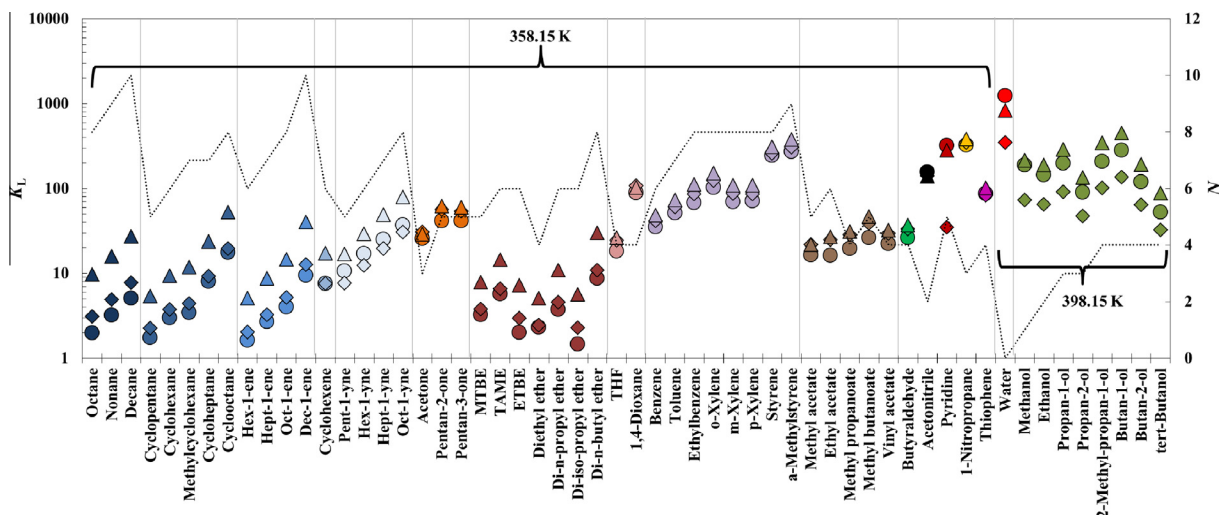


FIGURE 6. Experimental (gas + liquid) partition coefficients, K_L , for organic solutes and water in the ILs studied. \circ , $[\text{C}_4\text{mim}]\text{Cl}$; \diamond , $[\text{C}_4\text{mim}][\text{CH}_3\text{SO}_3]$; Δ , $[\text{C}_4\text{mim}][(\text{CH}_3)_2\text{PO}_4]$. The dotted line represents the number of carbons in the solutes structure, N . Symbols with the same color correspond to solutes of the same chemical family. (For interpretation of the references to color in this figure legend, the reader is referred to the web version of this article.)

$T = 358.15 \text{ K}$ is considerably low in all ILs studied suggesting the high potential for the extraction of acetonitrile from aliphatic hydrocarbons. In $[\text{C}_4\text{mim}][(\text{CH}_3)_2\text{PO}_4]$, also pyridine (1.18), 1-nitropropane (1.50) and thiophene (1.24) have low γ_{13}^∞ values at $T = 358.15 \text{ K}$, suggesting a high selectivity for the extraction of nitrogen and sulfur-containing compounds from alkanes.

The temperature dependence of γ_{13}^∞ is presented in the Supporting Information (figure S1). Increasing the temperature, a decrease in the natural logarithm of γ_{13}^∞ with the reciprocal temperature is observed for alkanes, cycloalkanes, alkenes, cycloalkenes, and few ethers. The inverse dependence is observed for all the other solutes, what will be hereafter taken into consideration.

According to Cláudio *et al.* [45], the polarity of the ILs studied follow the trend: $[(\text{CH}_3)_2\text{PO}_4]^- > \text{Cl}^- > [\text{CH}_3\text{SO}_3]^-$, in conformity with the relative values of γ_{13}^∞ observed for water and alcohols, the most polar solutes studied. Pyridine that is an aromatic ring with one methine group ($=\text{CH}-$) replaced by a nitrogen atom, also show the same behavior because of its high hydrogen bonding ability. The other organic solutes studied follow the trend: $[(\text{CH}_3)_2\text{PO}_4]^- > [\text{CH}_3\text{SO}_3]^- > \text{Cl}^-$.

TABLE 4
Density of the pure ILs studied as a function of temperature at 0.1 MPa.

T/K	$\rho/\text{g} \cdot \text{cm}^{-3a}$		
	$[\text{C}_4\text{mim}]\text{Cl}$	$[\text{C}_4\text{mim}][\text{CH}_3\text{SO}_3]$	$[\text{C}_4\text{mim}][(\text{CH}_3)_2\text{PO}_4]$
293.15			1.1665
298.15			1.1632
303.15			1.1594
308.15	1.0794		1.1562
313.15	1.0766		1.1527
318.15	1.0737		1.1495
323.15	1.0709		1.1461
328.15	1.0681		1.1430
333.15	1.0652	1.1506	1.1397
338.15	1.0624	1.1474	1.1365
343.15	1.0596	1.1443	1.1333
348.15	1.0569	1.1412	1.1301
353.15	1.0543	1.1379	1.1269
358.15	1.0517	1.1349	1.1237
363.15	1.0490	1.1319	1.1206
368.15	1.0464	1.1288	1.1174
373.15	1.0439	1.1258	

^a Standard uncertainties, u , are $u(\rho) = \pm 5 \cdot 10^{-4} \text{ g} \cdot \text{cm}^{-3}$, $u(T) = 0.02 \text{ K}$ and $u(p) = 0.05$.

4.2. Comparison with literature data

Similar studies have been published on solute infinite dilution activity coefficients in ILs. Figure 2 shows the experimental γ_{13}^∞ of several solutes in the ILs $[\text{C}_4\text{mim}]\text{Cl}$ and $[\text{C}_4\text{mim}][\text{CH}_3\text{SO}_3]$, and the respective literature values. To the best of our knowledge, no data are available for the IL $[\text{C}_4\text{mim}][(\text{CH}_3)_2\text{PO}_4]$. Analyzing figure 2, it can be seen that, in general, results are very consistent. The solutes THF and 1,4-dioxane are clear exception; THF in both ILs and 1,4-dioxane in $[\text{C}_4\text{mim}][\text{CH}_3\text{SO}_3]$, with more significant deviation to the literature values [46,47]. Additionally, our experimental data shows an increase in γ_{13}^∞ of toluene in $[\text{C}_4\text{mim}][\text{CH}_3\text{SO}_3]$, with increasing temperature, while the data reported by Stark *et al.* [47] shows the opposite trend. All the others aromatic hydrocarbons studied in this work, such as benzene, ethylbenzene, p-, m-, o-xylene, present the same slope observed for toluene. Moreover, for further comparison purposes data from literature involving ILs presenting the same cation, or one of the anions, were selected. Some standard organic solutes and the temperature of 358.15 K were chosen and are presented in table 3.

Regarding the anion chloride, increasing the alkyl chain length on the cation decreases considerably the γ_{13}^∞ with non-polar solvents. The same is observed for the non-polar solvents on the other anions studied suggesting that the increase on the cation alkyl chain enhances the dispersive interactions with the non-polar solvents. In comparison the effect on the polar compounds such as ethanol and water seems to be negligible, within the experimental uncertainty of the data, suggesting that for these compounds the dominant interactions are related to the anions and no longer with the cation.

4.3. Effect of the anion

As mentioned before, the anion has a large influence on the infinite dilution activity coefficients. In order to better understand this effect, some organic solutes with different characteristics were investigated. The (ion + dipole) interactions were studied using acetonitrile, to clarify the IL ability to solvate dipolar molecules. Octane and toluene allowed the investigation of σ -electron and π -electron dispersion forces, respectively. The hydrogen bond acceptor and donor properties of the ILs were investigated with propan-1-ol (a hydrogen bond donor) and 1,4-dioxane (a hydrogen

TABLE 5

Selectivities (S_{ij}^{∞}) and capacities (k_j^{∞}) at infinite dilution for different separation problems at $T = 358.15$ K.

Ionic liquids		$S_{ij}^{\infty}/k_j^{\infty}$			Reference
Cation	Anion	Octane/benzene	Cyclohexane/benzene	Cyclohexane/thiophene	
[C ₄ mim] ⁺	Cl ⁻	73.32/0.22	12.13/0.22	26.75/0.49	This work
	[CH ₃ SO ₃] ⁻	55.50/0.32	11.43/0.32	20.41/0.58	This work
	[(CH ₃) ₂ PO ₄] ⁻	20.58/0.43	5.28/0.43	9.88/0.80	This work
	[(CH ₃ (CH ₂) ₃) ₂ PO ₄] ⁻	7.20/1.17	3.06/1.17		[60] ^a
	[CF ₃ SO ₃] ⁻	30.61/0.61	8.16/0.61	11.27/0.85	[24]
[C ₈ mim] ⁺	Cl ⁻	13.67/0.80	6.04/0.80		[26] ^b
[C ₂ mim] ⁺	[CH ₃ SO ₃] ⁻	64.02/0.23 ^b	10.57 ^b /0.23 ^b	21.75/0.48	[32]
		86.08/0.24	12.18/0.24	24.59/0.49	[58] ^b
[C ₁ mim] ⁺	[(CH ₃) ₂ PO ₄] ⁻	65.71/0.27	10.58/0.27		[27] ^b
[C ₂ mim] ⁺	[(CH ₃ CH ₂) ₂ PO ₄] ⁻	36.24/0.43	10.70/0.43		[59] ^b
Other solvents					
Sulfolane		26.03/0.44			[61] ^a
NMP			4.49/-	-/0.93	[62] ^b

^a Interpolated value.^b Extrapolated value.

bond acceptor), respectively. The influence of the anion on the solvation properties of ILs was investigated with the three ILs studied in this work, [C₄mim]Cl, [C₄mim][CH₃SO₃] and [C₄mim][(CH₃)₂PO₄]. The effect of the nature of the anion on γ_{13}^{∞} of the organic solutes chosen is displayed in figure 3.

As can be seen, for acetonitrile, all γ_{13}^{∞} are very close, however chloride gives the larger value, followed by the anions methanesulfonate and dimethyl phosphate, where the dipole is better accommodated. Concerning 1,4-dioxane and propan-1-ol, the hydrogen bond acceptor and donor, it is possible to see that the choice of the anion has an important effect in the γ_{13}^{∞} values. The γ_{13}^{∞} of propan-1-ol decreases in the order of [CH₃SO₃]⁻ > Cl⁻ > [(CH₃)₂PO₄]⁻ by a factor close to 2. This sequence is in complete agreement to the rank based on the solvatochromic β parameter [48] for the description of the hydrogen bonding accepting ability of each anion. The γ_{13}^{∞} of 1,4-dioxane decreases according to Cl⁻ > [CH₃SO₃]⁻ > [(CH₃)₂PO₄]⁻. This happens because this solute can only interact with the cation ring's hydrogen atoms if they are not engaged in strong interactions with basic anions, and hence the activity coefficients are higher in the chloride-based IL. When comparing between the five solutes, the lower values of γ_{13}^{∞} in propan-1-ol attest the hydrogen-bond acceptor character of the anions chosen.

For the π and σ -electron dispersion forces the choice of the anion also plays a significant role. The lowest γ_{13}^{∞} of toluene, and hence the highest degree of interaction, is found for the [(CH₃)₂PO₄]⁻, followed by [CH₃SO₃]⁻ and Cl⁻. For octane the same trend was observed however, this solute shows higher γ_{13}^{∞} values and a higher variation between the different ionic liquids.

4.4. Thermodynamic functions at infinite dilution

The partial excess molar properties such as Gibbs energy, enthalpy, and entropy, all at infinite dilution, for the organic solutes and water in the studied ILs at the reference temperatures $T = (358.15 \text{ and } 398.15) \text{ K}$ (alcohols and water), were evaluated in order to provide more information about the interactions between the solutes and the ILs. The thermodynamic functions at infinite dilution, calculated through the γ_{13}^{∞} values are listed in Supporting Information (table S2) at the reference temperatures.

The $\overline{H}_m^{E,\infty}$, calculated through the temperature dependence of γ_{13}^{∞} (Eq. (6)), exhibit negative values for almost all solutes, expressing the favorable interactions between the solute and the solvent, with the exception of alkanes, cycloalkanes, alkenes, cycloalkenes and a few ethers, all apolar compounds, and the ILs. The $\overline{G}_m^{E,\infty}$ is positive for most of the solutes, with the exception of alcohols, water,

and acetonitrile (for [(CH₃)₂PO₄]⁻ and [CH₃SO₃]⁻), indicating strong interactions solute-IL for these polar solutes. The largest positive values of $\overline{G}_m^{E,\infty}$ are exhibited by aliphatic hydrocarbons, showing again the weak aliphatic hydrocarbon-IL interactions. Lastly, $\overline{S}_m^{E,\infty}$ are <0 for all solutes studied, indicating their reorganization inside the ionic liquid phase, and often representing the dominance of entropic effect over the enthalpic one.

In order to further understand the molecular level interactions in these systems, figure 4 relates γ_{13}^{∞} and partial molar excess properties, where three different areas can be distinguished. The region (II) corresponds to the (ILs + organic solutes) systems with positive deviations to Raoult's law, $\gamma_{13}^{\infty} > 1$ and, to some organic solutes also $\overline{G}_m^{E,\infty}$ and $\overline{H}_m^{E,\infty}$ are positive. In this region, mainly constituted by non-polar solutes such as alkanes, cycloalkenes, alkenes and a few ethers, no particular affinity between ILs and organic solutes molecules is expected. This low interaction between organic solutes and ILs can lead to the formation of immiscible solutions and consequently, phase separation. Thus, they may find themselves as potential solvents in (liquid + liquid) extraction, as will be shown below.

The region (III) corresponds to the (ILs + organic solutes) systems with negative deviations from Raoult's law ($\gamma_{13}^{\infty} < 1$) that is related to a spontaneous dissolution of organic solutes in the ILs. From all the solutes studied, only alcohols and water lie in this region, due to their strong polarity. All the partial excess molar properties studied are negative, revealing that the hydrogen bonding between organic solutes and the IL anions is much stronger than hydrogen bonding between solute and solute or (IL + IL) molecules, leading to an exothermic mixing behavior of these systems. As expected, systems with IL composed by the anion with stronger hydrogen basicity, [(CH₃)₂PO₄]⁻, exhibits lower values of $\overline{H}_m^{E,\infty}$.

Region (IV) presents $\gamma_{13}^{\infty} > 1$, $\overline{S}_m^{E,\infty}$ and $\overline{H}_m^{E,\infty} < 0 \text{ kJ} \cdot \text{mol}^{-1}$. This is the region where most organic solutes fall. For some solutes $\overline{G}_m^{E,\infty}$ is close to 0, while the enthalpic and entropic contributions are both negative, meaning that they cancel each other. As can be observed in figure 4, when region (IV) is compared to region (II) the dominance of the entropic term over the enthalpic is evident. It is also relevant to notice that when the interaction between the solute and IL are strong (regions I or III), the enthalpic effect is always dominant.

4.5. (Gas + liquid) partition coefficients

In order to calculate the (gas + liquid) partition coefficients, K_L , the ILs densities were measured over the temperature range from (293.15 to 373.15) K and the results are listed in table 4. Density

data were previously reported and are represented in figure 5, along with the experimental values from this work. As can be seen for the ILs $[\text{C}_4\text{mim}][(\text{CH}_3)_2\text{PO}_4]$ and $[\text{C}_4\text{mim}][\text{CH}_3\text{SO}_3]$ the experimental values are in good agreement with literature, with a maximum relative deviation of 0.11 and 0.08%, respectively. Concerning $[\text{C}_4\text{mim}]\text{Cl}$ more datasets are available, which show some inconsistencies within each other. Our data show very good agreement to those published by Machida *et al.* [49] and He *et al.* [50], presenting larger deviations to others [51–53]. However, taking in account the IL purity and water content, which sometimes are not given, discrepancies are not that significant, being the maximum relative deviation of 1.26% concerning the data of Kavitha *et al.* [52], for the IL $[\text{C}_4\text{mim}]\text{Cl}$ at $T = 313.15\text{ K}$.

The (gas + liquid) partition compares the affinity of the solute to both phases. Results are listed in Supporting Information (table S3) and presented in figure 6. As can be seen, for all solutes K_L decreases with increasing temperature, and increases with the alkyl chain in aliphatic and aromatic hydrocarbons, and ketones. The highest value is observed for water $K_L = 1233.27$ in $[\text{C}_4\text{mim}]\text{Cl}$ at $T = 358.15\text{ K}$, whereas the lowest value is observed for di-*iso*-propyl ether (0.99) in the same IL at $T = 388.15\text{ K}$. This is consistent with previous analyses, since higher K_L value corresponds to larger affinities of the solute to the liquid phase.

4.6. Selectivities and capacities

The measurements of the activity coefficients at infinite dilution can be used to evaluate the performance of ILs as solvents for several practical chemical separation problems [46,54,55]. This is achieved by the calculation of selectivities and capacities, parameters presented in Section 3. A suitable solvent should possess both a high selectivity and a high capacity for the components to be separated. The results obtained for S_{ij}^∞ and k_j^∞ , were calculated using Eqs. (9) and (10), and the results are presented in table 5, along with values from literature for ILs presenting the same anion or cation as those studied here. Some other important industrial solvents such as *N*-methyl-2-pyrrolidinone (NMP) and sulfolane are presented as well for comparison purposes.

Analyzing table 5 it is possible to see that the separation of octane/benzene is the easiest, especially with $[\text{C}_4\text{mim}]\text{Cl}$ and the methanesulfonate-based anions. The lowest values of selectivity are found for $[\text{C}_8\text{mim}]\text{Cl}$ and $[\text{C}_4\text{mim}][(\text{CH}_3(\text{CH}_2)_3)_2\text{PO}_4]$, both present a cation and an anion, respectively, with a longer alkyl chain. The cyclohexane/benzene separation problem is, according with the calculated values, the most difficult separation. As can be seen, selectivities are similar, but much lower than for the previous system. Despite the low capacity value the IL $[\text{C}_4\text{mim}]\text{Cl}$ is, once again, the one that makes the separation easier. Regarding the separation of sulfur compounds from aliphatic hydrocarbons, cyclohexane/thiophene, the values are similar among the studied ILs, but $[\text{C}_4\text{mim}]\text{Cl}$ is again the solvent presenting better selectivities. Common solvents, NMP and sulfolane, have lower values of selectivities in both aliphatic/aromatic separations than the ILs here studied.

Another very important problem is the de-nitrogenation of fuels. The values of selectivity for the separation of nitrogen compounds from aliphatic hydrocarbons as for example octane/pyridine or octane/1-nitropropane are (224.57, 15.63 and 40.57) and (131.54, 90.23 and 31.86) for Cl^- , $[\text{CH}_3\text{SO}_3]^-$ and $[(\text{CH}_3)_2\text{PO}_4]^-$, respectively, at $T = 358.15\text{ K}$. The values presented for the IL $[\text{C}_4\text{mim}]\text{Cl}$ are very promising.

5. Conclusions

In this work the activity coefficients at infinite dilution of ILs composed by the cation 1-butyl-3-methylimidazolium and the

anions chloride, methanesulfonate and dimethylphosphate were measured by (gas + liquid) chromatography techniques for 55 solutes and water, at four different temperatures. Comparisons with literature were carried out, showing consistent trends among the different ILs analyzed.

Thermodynamic functions at infinite dilution and (gas + liquid) partition coefficients were analyzed and it was concluded that the hydrogen bonding between organic solutes and the ILs anion plays a significant role on the interaction of the ILs with organic solutes, and determines the enthalpic behavior of the binary mixtures.

The ability of the ILs to act as entrainers in important separations was evaluated. In spite of the lower capacities obtained for the different separation processes studied, the selectivities achieved were quite high and, thus, these ILs could be used as an alternative separating agent for some typical separations.

Acknowledgements

This work was developed in the scope of the projects CICECO-Aveiro Institute of Materials (Ref. FCT UID/CTM/50011/2013), financed by national funds through the FCT/MEC and when applicable co-financed by FEDER under the PT2020 Partnership Agreement, and LSRE/LCM (Ref. FCT UID/EQU/50020/2013). This work was also supported by a STSM Grant from COST action CM1206. M.A.R.M thanks to FCT for financial support for the PhD Grant SFRH/BD/87084/2012 and to Andrzej Marciniak and Michał Wlazło for all the laboratorial support.

Appendix A. Supplementary data

Supplementary data associated with this article can be found, in the online version, at <http://dx.doi.org/10.1016/j.jct.2015.07.042>.

References

- [1] P.T. Anastas, P. Wasserscheid, A. Stark, Handbook of Green Chemistry, vol. 6, Green Solvents, Ionic Liquids, 2013.
- [2] S.J. Zhang, X.M. Lu, Q. Zhou, X. Li, X. Zhang, S. Lu, Ionic Liquids: Physicochemical Properties, first ed., Elsevier, Oxford – United Kingdom, 2009.
- [3] N.V. Plechkova, K.R. Seddon, Chem. Soc. Rev. 37 (2008) 123–150.
- [4] D. Holbrey, R.D. Rogers, R.A. Mantz, P.C. Trulove, V.A. Cocalia, A.E. Visser, J.L. Anderson, J.L. Anthony, J.F. Brennecke, E.J. Maginn, T. Welton, R.A. Mantz, Physicochemical Properties, Ionic Liquids in Synthesis, Wiley-VCH Verlag GmbH and Co. KGaA, 2008 (pp. 57–174).
- [5] D. Han, K.H. Row, Molecules 15 (2010) 2405–2426.
- [6] B. Kirchner, Ionic Liquids, Topics in Current Chemistry, Springer, Heidelberg, Germany, 2010.
- [7] U. Domanska, A. Pobudkowska, F. Eckert, Green Chem. 8 (2006) 268–276.
- [8] U. Domańska, E.V. Lukoshko, M. Królkowski, Fluid Phase Equilib. 345 (2013) 18–22.
- [9] C.F. Poole, J. Chromatogr. A 1037 (2004) 49–82.
- [10] T.M. Letcher, A. Marciniak, M. Marciniak, J. Chem. Eng. Data 50 (2005) 1294–1298.
- [11] A. Heintz, L.M. Casás, I.A. Nesterov, V.N. Emelyanenko, S.P. Verevkin, J. Chem. Eng. Data 50 (2005) 1510–1514.
- [12] A. Marciniak, M. Wlazło, J. Chem. Thermodyn. 64 (2013) 114–119.
- [13] J. Canongia Lopes, A.H. Pádua, Theoret. Chem. Acc. 131 (2012) 1–11.
- [14] E.J. Maginn, J. Phys.: Condens. Matter 21 (2009) 373101–373118.
- [15] M. Sellin, B. Ondruschka, A. Stark, Hydrogen Bond Acceptor Properties of Ionic Liquids and Their Effect on Cellulose Solubility, Cellulose Solvents: For Analysis, Shaping and Chemical Modification, American Chemical Society, 2010 (pp. 121–135).
- [16] Y. Danten, M.I. Cabaço, M. Besnard, J. Phys. Chem. A 113 (2009) 2873–2889.
- [17] I. Khan, M. Taha, P. Ribeiro-Claro, S.P. Pinho, J.A.P. Coutinho, J. Phys. Chem. B 118 (2014) 10503–10514.
- [18] P.J. Carvalho, I. Khan, A. Morais, J.F.O. Granjo, N.M.C. Oliveira, L.M.N.B.F. Santos, J.A.P. Coutinho, Fluid Phase Equilib. 354 (2013) 156–165.
- [19] M.G. Freire, L.M.N.B.F. Santos, I.M. Marrucho, J.A.P. Coutinho, Fluid Phase Equilib. 255 (2007) 167–178.
- [20] A.R. Ferreira, M.G. Freire, J.C. Ribeiro, F.M. Lopes, J.G. Crespo, J.A.P. Coutinho, Indust. Eng. Chem. Res. 50 (2011) 5279–5294.
- [21] C.M.S.S. Neves, J.F.O. Granjo, M.G. Freire, A. Robertson, N.M.C. Oliveira, J.A.P. Coutinho, Green Chem. 13 (2011) 1517–1526.

- [22] L.M.C. Pereira, M.B. Oliveira, F. Llovel, L.F. Vega, J.A.P. Coutinho, J. Supercrit. Fluids 92 (2014) 231–241.
- [23] U. Domańska, E.V. Lukoshko, J. Chem. Thermodyn. 66 (2013) 144–150.
- [24] U. Domańska, A. Marciniak, J. Phys. Chem. B 112 (2008) 11100–11105.
- [25] A. Heintz, S.P. Verevkin, J. Chem. Eng. Data 50 (2005) 1515–1519.
- [26] W. David, T.M. Letcher, D. Ramjugernath, J. David Raal, J. Chem. Thermodyn. 35 (2003) 1335–1341.
- [27] R. Kato, J. Gmehling, Fluid Phase Equilib. 226 (2004) 37–44.
- [28] M. Krummen, P. Wasserscheid, J. Gmehling, J. Chem. Eng. Data 47 (2002) 1411–1417.
- [29] P. Wasserscheid, T. Welton, Ionic Liquids in Synthesis, second ed., Wiley-VCH Verlag GmbH & Co. KGaA, Darmstadt, Federal Republic of Germany, 2009.
- [30] U. Domańska, M. Królikowska, J. Phys. Chem. B 114 (2010) 8460–8466.
- [31] U. Domańska, M. Królikowski, W.E. Acree Jr, G.A. Baker, J. Chem. Thermodyn. 58 (2013) 62–69.
- [32] U. Domańska, M. Królikowski, J. Chem. Thermodyn. 54 (2012) 20–27.
- [33] U. Domańska, M. Królikowski, J. Chem. Eng. Data 55 (2010) 4817–4822.
- [34] U. Domańska, A. Marciniak, J. Phys. Chem. B 111 (2007) 11984–11988.
- [35] U. Domanska, A. Marciniak, J. Chem. Thermodyn. 40 (2008) 860–866.
- [36] P.J. Carvalho, T. Regueira, L.M.N.B.F. Santos, J. Fernandez, J.A.P. Coutinho, J. Chem. Eng. Data 55 (2009) 645–652.
- [37] D.H. Everett, Trans. Faraday Soc. 61 (1965) 1637–1645.
- [38] A.J.B. Cruickshank, B.W. Gaaney, C.P. Hicks, T.M. Letcher, R.W. Moody, C.L. Young, Trans. Faraday Soc. 65 (1969) 1014–1031.
- [39] D.W. Grant, Gas–Liquid Chromatography, van Nostrand Reinhold, London, UK, 1971.
- [40] Design Institute for Physical Properties, Sponsored by AIChE (2005; 2008; 2009; 2010). DIPPR Project 801 – Full Version. Design Institute for Physical Property Research/AIChE. Online version available at: <http://knovel.com/web/portal/browse/display?_EXT_KNOVEL_DISPLAY_bookid=1187&VerticalID=0>.
- [41] B.E. Poling, J.M. Prausnitz, Properties of Gases and Liquids, McGraw-Hill Publishing, 2001.
- [42] U. Domańska, A. Marciniak, J. Phys. Chem. B 114 (2010) 16542–16547.
- [43] A. Stark, Ionic liquid structure-induced effects on organic reactions, in: B. Kirchner (Ed.), Ionic Liquids, Springer, Berlin Heidelberg, 2010, pp. 41–81.
- [44] A.A.H. Pádua, M.F. Costa Gomes, J.N.A. Canongia Lopes, Acc. Chem. Res. 40 (2007) 1087–1096.
- [45] A.F.M. Claudio, L. Swift, J.P. Hallett, T. Welton, J.A.P. Coutinho, M.G. Freire, Phys. Chem. Chem. Phys. 16 (2014) 6593–6601.
- [46] C. Jork, C. Kristen, D. Pieraccini, A. Stark, C. Chiappe, Y.A. Beste, W. Arlt, J. Chem. Thermodyn. 37 (2005) 537–558.
- [47] A. Stark, B. Ondruschka, D.H. Zaitsau, S.P. Verevkin, J. Chem. Eng. Data 57 (2012) 2985–2991.
- [48] Y.-H. Gong, C. Shen, Y.-Z. Lu, H. Meng, C.-X. Li, J. Chem. Eng. Data 57 (2012) 33–39.
- [49] H. Machida, R. Taguchi, Y. Sato, J.R.L. Smith, J. Chem. Eng. Data 56 (2011) 923–928.
- [50] R.-H. He, B.-W. Long, Y.-Z. Lu, H. Meng, C.-X. Li, J. Chem. Eng. Data 57 (2012) 2936–2941.
- [51] V. Govinda, P. Attri, P. Venkatesu, P. Venkateswarlu, Fluid Phase Equilib. 304 (2011) 35–43.
- [52] T. Kavitha, T. Vasantha, P. Venkatesu, R.S. Rama Devi, T. Hofman, J. Mol. Liq. 198 (2014) 11–20.
- [53] J.G. Huddleston, A.E. Visser, W.M. Reichert, H.D. Willauer, G.A. Broker, R.D. Rogers, Green Chem. 3 (2001) 156–164.
- [54] G. Wytze Meindersma, A. Podt, A.B. De Haan, Fuel Process. Technol. 87 (2005) 59–70.
- [55] Z. Lei, W. Arlt, P. Wasserscheid, Fluid Phase Equilib. 241 (2006) 290–299.
- [56] U. Domańska, E. Bogel-Łukasik, R. Bogel-Łukasik, Chem. – A Eur. J. 9 (2003) 3033–3041.
- [57] A. Stark, A.W. Zidell, J.W. Russo, M.M. Hoffmann, J. Chem. Eng. Data 57 (2012) 3330–3339.
- [58] J.-C. Moïse, F. Mutelet, J.-N. Jaubert, L.M. Grubbs, W.E. Acree, G.A. Baker, J. Chem. Eng. Data 56 (2011) 3106–3114.
- [59] M.-L. Ge, J.-B. Chen, J. Chem. Eng. Data 56 (2011) 3183–3187.
- [60] M.L. Ge, X.J. Song, G.M. Li, Y.H. Li, F.Z. Liu, H.L. Ma, J. Chem. Eng. Data 57 (2012) 2109–2113.
- [61] Y.-X. Yu, Q. Gong, L.-L. Huang, J. Chem. Eng. Data 52 (2007) 1459–1463.
- [62] M. Krummen, D. Gruber, J. Gmehling, Ind. Eng. Chem. Res. 39 (2000) 2114–2123.